Porous hydroxyapatite-polyhydroxybutyrate composites fabricated by a novel method via centrifugation

Michael M Porter[1], Steve Lee[1], Nuttapol Tanadchangsaeng[2], Matt J Jaremko[2], Jian Yu[2], Marc Meyers[1,3], Joanna McKittrick[1,3]

[1]*Materials Science and Engineering Program, University of California, San Diego, 9500 Gilman Dr., La Jolla, CA, 92093, USA;*
[2]*Hawaii Natural Energy Institute, University of Hawai´i at Mānoa, 1680 East West Road, POST 109, Honolulu, HI, 98622, USA;*
[3]*Department of Mechanical and Aerospace Engineering, University of California, San Diego, 9500 Gilman Dr., La Jolla, CA, 92093, USA.*

ABSTRACT

Porous hydroxyapatite-polyhydroxybutyrate (HA-PHB) composites were fabricated by infiltrating PHB micro-/nano-particles into rigid HA scaffolds via centrifugation, followed by subsequent heating at 175°C to melt the PHB into the scaffolds. HA scaffolds were obtained by heating trabecular bovine femur bone at 1350°C to remove the organic and sinter the HA. PHB particles were recovered and purified from microbial cells by two different chemical methods, which either *filled* the apparent porosity of the scaffolds or *coated* the trabecular network of the scaffolds after heating. The mechanical properties, porosity, HA/PHB volume fractions and surface adhesion of the resulting HA-PHB composites were investigated and compared to the original HA scaffolds. The final porosities of the filled and coated composites were ~54% and ~67%, respectively. All of the HA-PHB composites showed a slight increase in strength with the addition of PHB. The filled composites showed no change in stiffness from the addition of PHB, while the coated composites showed an increase in stiffness over the original HA scaffolds from ~ 35 MPa to ~ 105 MPa. The enhanced stiffness in the coated composites was due to strong interactions between its HA and PHB constituent phases. Very little inter-constituent adhesion was observed in the filled composites.

INTRODUCTION

The fabrication of new biocompatible composites that mimic the biological, structural and mechanical properties of natural materials, such as bone, are of great interest in the fields of tissue engineering, materials science and mechanical engineering. Bone is a natural inorganic-organic composite material primarily composed of hydroxyapatite (HA) and collagen [1, 2]. Bone is a low density, highly porous material with higher than expected strength, stiffness, and toughness [1-3]. The exceptional mechanical properties in bone are due to its complex structural hierarchy at multiple length scales and the strong interactions that exist between its individual mineral and protein constituents [1-3]. New materials that mimic the natural architecture and match the mechanical properties of bone may be useful in a variety of tissue engineering applications, such as total bone replacements, bone substitutes, and bone implant scaffolds.

A variety of bone implant materials currently exist [4-8]. Some of the most promising materials are composites composed of hydroxyapatite (HA) - the primary mineral constituent in bone - and polymers such as polylactic acid (PLA), polyglycolic acid (PGA), polycaprolactone (PCL), or polyhydroxyalkanoate (PHA) [9-17]. HA-biopolymer composites are attractive because they are biocompatible, osteoconductive/inductive, and biodegradable/resorbable. Most HA-biopolymer composites developed to date, however, are simple mixtures of HA powders or whiskers dispersed throughout a biopolymer matrix. A major disadvantage of these composites is their inherent lack of porosity and structural order. A novel way to fabricate HA-biopolymer composites that mimic the complex microstructures in bone is to infiltrate a polymeric phase into rigid HA scaffolds. Two important design considerations for the fabrication of this type of composite include: (1) the architectural design of the HA scaffold and (2) the polymer infiltration technique. HA scaffolds can be found in nature [1, 18] or designed synthetically by a variety of methods [19-24]. Polymer infiltration techniques that currently exist including polymer melt immersion [25], polymer-solvent evaporation [26-28], *in situ* polymerization [29, 30], and chemical vapor deposition [31].

This work introduces for the first time, polymer infiltration via centrifugation as a low cost, mechanically driven technique to infiltrate biopolymer micro-/nano-particles into rigid HA scaffolds.

This study aims to develop porous HA-polyhydroxybutyrate (PHB) composites with enhanced mechanical properties and similar trabecular architecture to that of natural cancellous bone. PHB is a type of PHA biopolyester that accumulates naturally in microbial cells as tiny intracellular granules. In its purified form PHB is a rigid, highly crystalline (~80 %) biopolymer, making it ideal for compressive load-bearing applications [14, 17]. Micro-/nano-particles of PHB may be recovered from its host cells by extracting and purifying the biopolyester with a variety chemical methods [32-35]. In this work, trabecular HA scaffolds from deproteinated bovine femur bone were infiltrated with PHB particles via centrifugation and heated to melt the biopolyester into the HA scaffolds. Two different chemical methods were used to recover PHB particles, which resulted in two very different HA-PHB composites. In one case PHB filled the apparent porosity of the HA scaffolds, while in the other case PHB coated the trabecular network of the HA scaffolds. The physical and mechanical properties of the different HA-PHB composites were characterized and compared to that of the original HA scaffolds with microscopy imaging and compression testing.

MATERIALS AND METHODS

HA scaffolds

The HA scaffolds were obtained from trabecular bone from the proximal end of a bovine femur bone (~18 months old) sourced from a local supermarket. For sample preparation, the soft tissues were removed from the bone and the remaining bone marrow was cleaned with a dental water pick. The cleaned bone was then cut into small samples approximately 5×5×7 mm^3. The samples were heated in a high temperature furnace at 1350 °C for 3 hrs at ramp and cool down rates of ± 5 °C/min to remove the organic and sinter the remaining HA into rigid scaffolds (Fig 1A). These scaffolds retained their original trabecular microstructure with pore sizes ranging from 100-500 μm in diameter and were composed of 100 % hydroxyapatite - confirmed by X-ray diffraction (XRD) on a Miniflex II XRD machine (Rigaku, The Woodlands, TX). Four sets of 8 samples (32 total scaffolds) with similar dry mass and volume were selected for this study, so that the initial density (ρ = 0.48 ± 0.03 g/cm^3) and porosity (ϕ = 84.7 ± 0.9 %) of all the samples tested were nearly equal.

Recovery of PHB particles

An aqueous solution (pH 7) of *Ralstonia eutropha* cells containing 65 wt% PHB was centrifuged at 5000 g for 20 min and then resuspended in 0.2 M H_2SO_4 (pH 2.0) to stop cell activity. The acidic solution of cells contained 200 g/L dry cell mass and 75 wt% PHB. The acidic solution of cells was subjected to two different chemical recovery methods: (1) pH change and (2) acetone cleaning. In the pH method, the acidic solution of cells was heated at 100°C for 1 hr, then the pH of the solution was raised to 12 by adding 10 M NaOH and heated at 100 °C for 10 min. The basic solution of cells was then centrifuged at 7500 g for 10 min to remove the majority of non-PHB cell debris in the supernatant. In the acetone method, the acidic solution of cells was centrifuged at 7500 g for 10 min, resuspended in 200 vol% acetone and stirred for 24 hr. The treated slurry was then centrifuged at 7500 g for 10 min to remove the majority of cell debris in the supernatant. The pellets containing PHB particles from both methods were each suspended separately in a commercially available bleach solution of 6 wt% NaClO, stirred for 1 hr, and centrifuged to remove any residual biomass. The PHB particles from each solution were again each resuspended in 6 wt% NaClO twice more, then washed three times with deionized water and oven dried at 60 °C to ensure recovery of high purity PHB particles. The PHB particles recovered by the two methods were both confirmed to be > 99.9 % pure PHB, determined by gas chromatography with a Varian 450-GC analyzer (Varian, Inc., Walnut Creek, CA). The particle size distributions of the PHB recovered by the two methods were analyzed with a 90Plus/BI-MAS particle size analyzer (Brookhaven Instruments Corporation, Holtsville, NY) capable of measuring particles in the range of 2 nm to 3 μm.

Fabrication of HA-PHB composites

The PHB particles recovered from each method (i.e., pH and acetone) and an even mixture of PHB particles from both methods (pH/acetone, 1/1 by volume) were infiltrated into the sintered HA scaffolds via centrifugation. First, dried PHB particles from each case were suspended in water for working concentrations of ~50 g/L and ball-milled with alumina grinding media for 30 min to thoroughly mix the solutions and break apart any large aggregates of particles. Second, HA

scaffolds were placed in flat bottomed centrifuge tubes and ~10 mL of the PHB particle solutions were pipetted over the scaffolds. Third, the centrifuge tubes containing the HA scaffolds and PHB particle solutions were spun at 5000 g for 10 min to infiltrate the PHB particles into the porous scaffolds. Then, the supernatant was removed, replaced with a fresh solution of PHB particles, and centrifuged. The process was repeated until the scaffolds were completely covered by a pellet of PHB particles. After complete infiltration, the centrifuge tubes containing the wet pellets were oven dried overnight at 60 °C. After drying, excess PHB was carefully removed from the HA-PHB pellets. Finally, the dried HA-PHB pellets (Fig 1B) were placed in an open atmosphere oven at 175 °C for 30 min to melt the PHB particles into the HA scaffolds, then cooled at room temperature. A heating temperature of 175 °C was selected to limit PHB degradation, since the melting and molecular degradation points of PHB are nearly equal at ~180 °C [36].

Physical characterization

Density and porosity measurements were calculated from the dry weight and volume of the samples with respect to the known densities of pure HA ($\rho_{HA}^{'} = 3.14$ g/cm^3) [1] and pure PHB ($\rho_{PHB}^{'} = 1.22$ g/cm^3) [37]. The volume fractions (φ_i) of the HA and PHB constituents were calculated by equations 1 and 2:

$$\varphi_{HA} = \frac{V_{HA}}{V} = \frac{m_{HA\,scaffold}/\rho_{HA}^{'}}{V} \quad (1)$$

$$\varphi_{PHB} = \frac{V_{PHB}}{V} = \frac{(m_{HA{\cdot}PHB\,composite} - m_{HA\,scaffold})/\rho_{PHB}^{'}}{V} \quad (2)$$

where V is the total volume of the porous rectangular cuboid samples, m_i is the mass and V_i is the volume of the HA scaffold, HA-PHB composite, HA and PHB fractions, respectively. The porosity (ϕ) of the samples were calculated by equation 3:

$$\phi = 1 - \varphi_{HA} - \varphi_{PHB}\ . \quad (3)$$

Microscopy

Optical microscopy images were taken with a VHX-1000 digital microscope system equipped with a CCD camera (KEYENCE Corporation, Osaka, Japan).

Transmission electron microscopy (TEM) images were viewed on a LEO912 EFTEM (Zeiss, Germany) at 100 kV and photographed with a frame-transfer CCD camera (Proscan, Germany). For TEM preparation the cells were fixed with glutaraldehyde and calcium chloride in a sodium cacodylate buffer, then post-fixated with osmium tetroxide, stained with uranyl acetate, dehydrated with ethanol and embedded in epoxy. Ultrathin (60-80 nm) sections were obtained on an Ultracut E ultramicrotome (Reichert, Austria), double stained with uranyl acetate and lead citrate.

Scanning electron microscopy (SEM) images were taken at 5 kV on a Philips XL30 field emission environmental scanning electron microscope (ESEM) (FEI-XL30, FEI Company, Hillsboro, OR). For SEM preparation the samples were sputter-coated with iridium using an Emitech K575X sputter coater (Quorum Technologies Ltd., West Sussex, UK).

Mechanical testing

Compression testing of the samples was performed on an Instron materials testing machine (Instron 3342, Norwood, MA) with a 500 N load cell at a crosshead velocity of 10^{-3} mm/sec. The compressive strength and elastic modulus were determined from the maximum stress and the linear slope of the stress-strain curve just before the maximum stress, respectively. The relative strength and modulus were calculated by dividing the measured values by the strength and modulus of fully dense HA ($\sigma_{HA}^{'} = 800$ MPa, $E_{HA}^{'} = 112$ GPa) [1].

RESULTS AND DISCUSSION

Fig 1 shows representative images of a sintered HA scaffold before centrifugation (Fig 1A) and after centrifugation with infiltrated PHB particles (Fig 1B). As seen in the figure, the PHB particles completely filled the apparent porosity of the HA scaffolds.

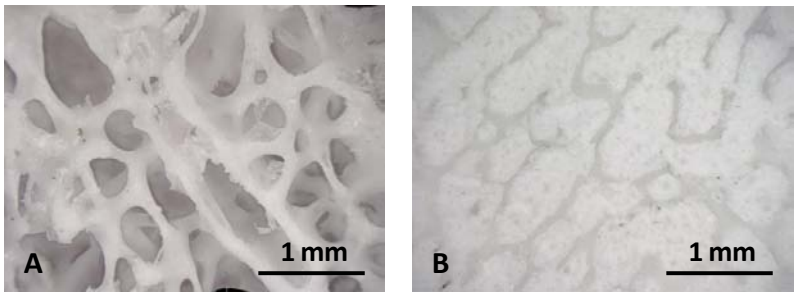

Fig 1. Images of a sintered HA scaffold: **(A)** before polymer infiltration showing the porous scaffold and **(B)** after polymer infiltration showing PHB particles completely filling the scaffold.

Fig 2 shows representative TEM micrographs of the progression of PHB particles at different stages of polymer recovery by the pH method. During recovery, the PHB particles were extracted from the cells and residual non-PHB biomass was removed. *In vivo*, PHB is amorphous and exists in the cells as discrete, intracellular granules 200-500 nm in diameter (Fig 2A). As the amorphous granules are extracted from the cells they tend to aggregate into larger particles (Fig 2B-C). However, varying degrees of crystallization may occur in the particles depending on the particular recovery method used [36, 38]. Highly crystalline particles are less likely to aggregate. Therefore, inducing PHB crystallization is desirable to recover submicron sized particles [36]. Fig 3 shows the particle size distribution of the PHB particles recovered by the pH and acetone methods. As seen in the figure, the pH and acetone methods yielded particles with average diameters of 617 ± 49 nm and 896 ± 94 nm, respectively.

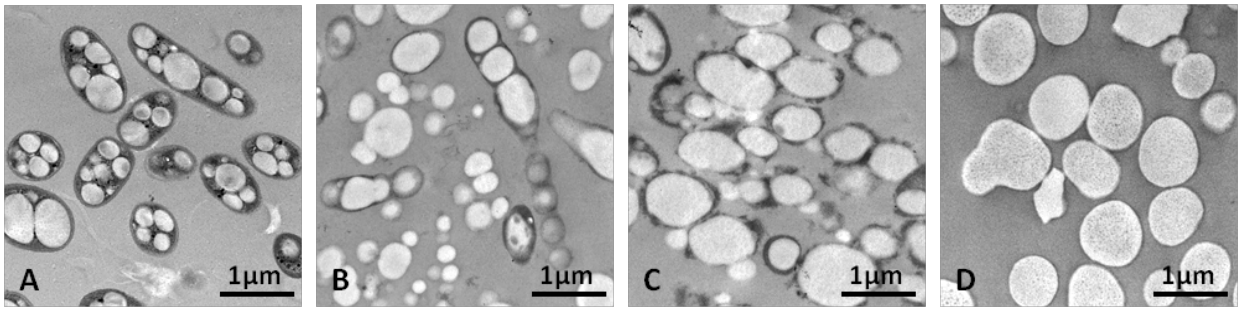

Fig 2. TEM images of PHB particles at different stages of recovery by the pH method: **(A)** *in vivo* at pH 7; **(B-C)** after partial polymer recovery; **(D)** after complete polymer recovery.

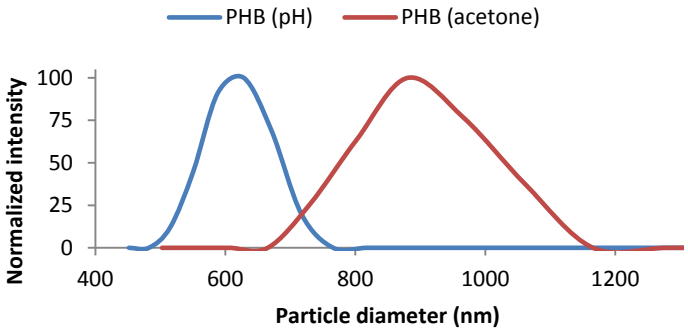

Fig 3. Particle size distribution of the PHB particles recovered by the pH method (blue) and acetone method (red).

Depending on the PHB particles used to infiltrate the scaffolds (i.e., pH, acetone, or mixed), the physical and mechanical properties of the resulting HA-PHB composites were quite different. Fig 4 shows representative images of the HA-PHB composites fabricated by heating the scaffolds infiltrated with PHB from the three different particle solutions. Fig 5 shows the HA-PHB interfaces at fracture surfaces of the three different composites. As seen in Fig 4A and 5A, the PHB particles recovered by the pH method filled the large pores of the HA scaffolds, but did not seem to wet and adhere to the surfaces of the trabecular network after heating. Fig 4B and 5B show that the PHB particles recovered by the acetone method fully coated the trabecular network of the HA scaffolds after heating. A mixture of the PHB particles recovered by both the pH and acetone methods filled the pores of the HA scaffolds and seemed to adhere to very little of the HA scaffold surfaces after heating, as seen in Fig 4C and 5C.

The exact mechanisms that lead to the different wetting behaviors of PHB (i.e., filling or coating the scaffolds) are not well understood at this point. It seems that the particular chemical treatments used to recover the PHB particles may, not only affect the PHB particle size, but also the thermodynamic and electrochemical properties of the PHB particles. It was determined that the three different solutions of PHB particles all had a pH in the range of 4-5. Lowering or raising the pH of the solutions had no effect on the wetting behavior of the particles; although, a significant decrease in the strength and modulus of the resulting composites were observed from solutions prepared at high pH (data not shown here). This observation can be explained by the fact that increasing the pH of the PHB particle solutions causes significant molecular degradation in the PHB, thereby resulting in the poor mechanical properties of the composites.

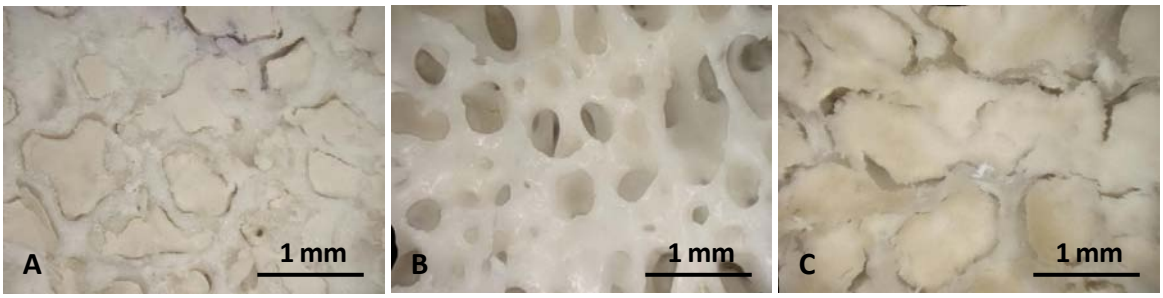

Fig 4. Images of HA-PHB composites: **(A)** PHB recovered by the pH method filling the porous scaffold; **(B)** PHB recovered by the acetone method coating the trabecular scaffold; **(C)** a mixture of PHB recovered by both the pH and acetone methods filling the porous scaffold.

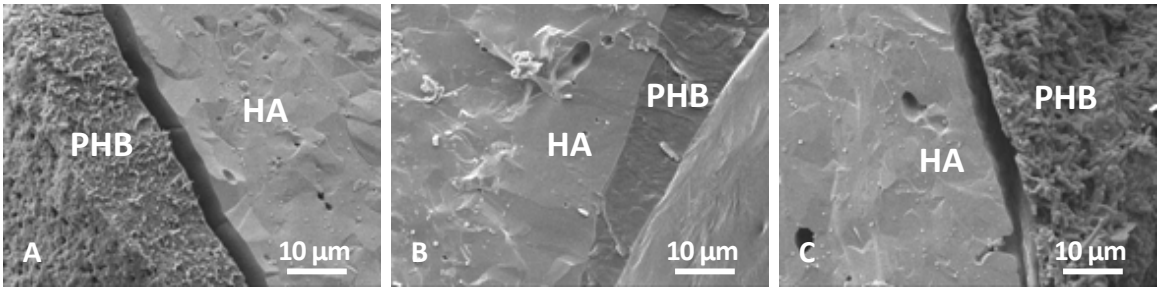

Fig 5. SEM micrographs of the composite fracture surfaces showing the HA-PHB interfaces: **(A)** HA filled with PHB recovered by the pH method; **(B)** HA coated with PHB recovered by the acetone method; **(C)** HA filled with PHB recovered by both methods (mixed).

Fig 6 contains plots comparing the physical and mechanical properties of the original sintered HA scaffolds before polymer infiltration and the HA-PHB composites filled or coated with PHB recovered by the pH, acetone, and mixed methods. For clarity, the four different specimens are referred to as HA, HA-PHB (pH), HA-PHB (acetone), and HA-PHB (mixed), corresponding to the images in Fig 1A and Fig 4A-C, respectively. As seen in Fig 6A the volume fraction of the HA is nearly equal for all the specimens tested (~15 vol% HA). The volume fraction of the PHB and porosity of the HA-PHB composites, however, varies. The HA-PHB (pH) and HA-PHB (mixed) composites filled with PHB both have larger PHB fractions (~30 vol% PHB) than the HA-PHB (acetone) composite coated with PHB (~17 vol% PHB). Accordingly, the porosity of the HA-PHB (acetone) composite coated with PHB has a greater porosity (~67 %) than the HA-PHB (pH) and HA-PHB (mixed) composites filled with PHB (~54 %). Dry weight measurements of the composites before and after heating confirmed that there was no significant loss of PHB from heating at 175 °C. The lower volume fraction of PHB in the HA-PHB (acetone)

composite is due to the larger particle sizes of the PHB recovered by acetone (Fig 3), which reduces the amount of PHB that can be packed into the pores of the HA scaffolds.

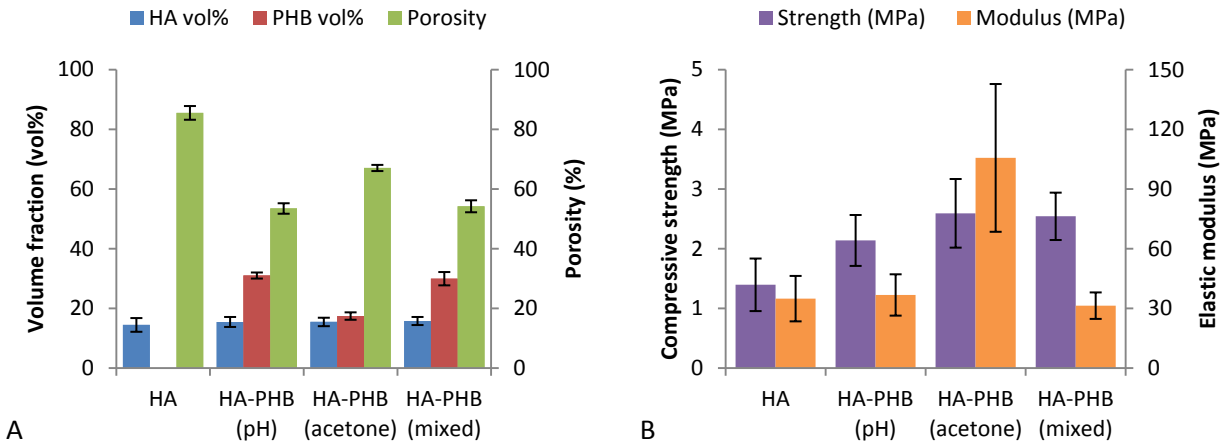

Fig 6. Comparison of the HA scaffold, HA-PHB (pH), HA-PHB (acetone), and HA-PHB (mixed) composites filled or coated with PHB. **(A)** Volume fractions of HA (blue) and PHB (red) and the final porosity of the scaffolds/composites (green); **(B)** Compressive strength (purple) and elastic modulus (orange) of the scaffolds/composites. Error bars show the true standard deviation of the mean (sample size for each specimen, N = 8).

Fig 6B compares the compressive mechanical properties of the HA scaffold with the three HA-PHB composites fabricated in this study. As seen in the plot the compressive strengths of the composites (~2.5 MPa) are slightly greater than the HA scaffolds (~1.5 MPa). The compressive elastic modulus of the composites, however, did not follow a similar trend. Interestingly, the composites *filled* with PHB (i.e., pH and mixed) did not show any increase in stiffness, while the composite *coated* with PHB (i.e., acetone) showed a significant increase in stiffness over the HA scaffold from ~35 MPa to ~105 MPa. The small increase in strength seen in all the composites can be attributed to the addition of PHB. As seen in Fig 7A, the strengths of the HA scaffolds and the HA-PHB composites relative to pure HA are strongly dependent on the volume fraction of the HA material. Adding PHB to the composites increased their strength and decreased their dependence on the HA phase. The relative stiffness of the composites, on the other hand, seemed to become more dependent on the volume fraction of the HA phase when PHB was added (Fig 7B). Moreover, the degree of interaction between the individual HA and PHB constituent phases seemed to be most influential on the resulting composite stiffness. The strong interaction between the PHB coating and the HA struts of the trabecular network in the HA-PHB (acetone) composite (Fig 5B) resulted in much higher stiffness than the other two composites filled with PHB, where very little inter-constituent contact was observed (Fig 5A and 5C). This explains why the *coated* HA-PHB (acetone) composite was much stiffer yet more porous than the *filled* HA-PHB (pH and mixed) composites. These results agree with similar observations made in nature, where the strong interactions between individual constituent phases enhance mechanical properties regardless of a material's low density and high porosity. Table 1 summarizes the porosity (ϕ), strength (σ), modulus (E), and the slopes (m, n) of fitted trend lines determined from Fig 7, corresponding to equations 4 and 5, modified from Gibson and Ashby [39]:

$$\frac{\sigma}{\sigma'_{HA}} = C_1(\varphi_{HA})^m \tag{4}$$

$$\frac{E}{E'_{HA}} = C_2(\varphi_{HA})^n \tag{5}$$

where σ and E are the measured compressive strength and modulus of the samples, $\sigma'_{HA} = 800$ MPa and $E'_{HA} = 112$ GPa for fully dense HA [1], φ_{HA} is the volume fraction of HA in the samples, C_1 and C_2 are empirical constants, and m and n are the slopes of the power law fits. As seen in the Table 1, m decreases and n increases when PHB is added to the HA scaffolds.

This result agrees with the conclusion that the rigid microstructure of the HA scaffolds plays a more significant role in adding stiffness to the composites, while the addition of PHB adds strength.

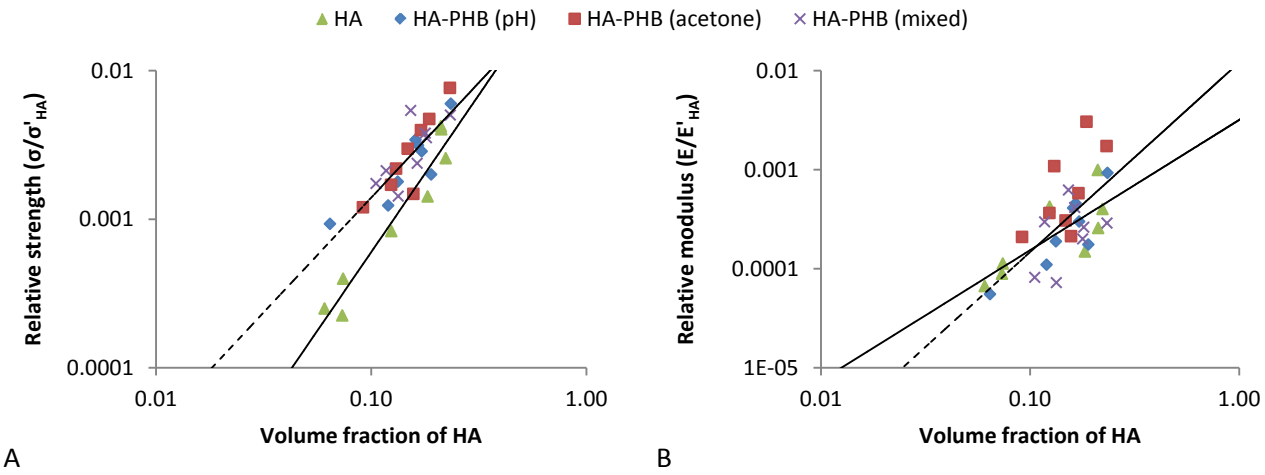

Fig 7. Comparison of the HA scaffolds, HA-PHB (pH), HA-PHB (acetone), and HA-PHB (mixed) composites filled or coated with PHB. **(A)** Relative compressive strength versus volume fraction of HA; **(B)** Relative elastic modulus versus volume fraction of HA. Trend lines show power law fits for the HA scaffolds (solid) and HA-PHB composites (dashed).

Table 1. Porosity, mechanical properties, and slopes of the power law fits from Fig 6 for the HA scaffolds and HA-PHB composites

Sample	*PHB*	Porosity (%)	Strength (MPa)	Modulus (MPa)	*m*	*n*
HA scaffold	---	85.5 ± 2.3	1.40 ± 0.44	34.93 ± 11.41	2.11	1.32
HA-PHB (pH)	*filled*	53.5 ± 1.8	2.14 ± 0.43	36.79 ± 10.38	1.33	1.98
HA-PHB (acetone)	*coated*	67.1 ± 1.0	2.59 ± 0.57	105.65 ± 37.13	2.00	2.34
HA-PHB (mixed)	*filled*	54.2 ± 2.0	2.54 ± 0.40	31.41 ± 6.66	1.43	1.32

* All values stated as average ± standard deviation.

CONCLUSIONS

Hydroxyapatite-polyhydroxybutyrate (HA-PHB) composites fabricated by infiltrating deproteinized, sintered trabecular bone scaffolds with PHB micro-/nano-particles via centrifugation were analyzed and compared. Depending on the chemical methods used to recover the PHB particles, the PHB either filled or coated the HA scaffolds after polymer infiltration and heating at 175 °C. All of the HA-PHB composites showed a slight increase in strength with the addition of PHB. The *filled* composites showed no change in stiffness from the addition of PHB, while the *coated* composites showed a dramatic increase in stiffness over the original HA scaffolds from ~35 MPa to ~105 MPa. Regardless of the higher porosity observed in the coated composites, strong interactions between its individual HA and PHB constituent phases seemed to be the underlying reason for its enhanced stiffness.

The HA-PHB composites develop in this work are fully biocompatible materials that may be useful in tissue engineering applications such as bone implant scaffolds. When fabricating bone implants it is desirable to make scaffolds with high porosity and large pore sizes that allow the migration, adhesion, and proliferation of cells such as osteoblasts to promote bone ingrowth. The biocompatibility, large pore sizes, high porosity, and natural trabecular architecture of the coated HA-PHB composites designed in this work may be ideal scaffold environments for the development of new tissues and bone ingrowth. Still, additional research on the exact mechanisms related to the fabrication and mechanical performance of these scaffolds is necessary before *in vitro* or *in vivo* implantation. It is important to understand why the PHB particles recovered by the two different methods either filled or coated the surfaces of the HA scaffolds. It is also necessary to optimize the fabrication process of the composites to further enhance HA-PHB interfacial adhesion and improve the compressive mechanical properties of the resulting composites.

ACKNOWLEDGEMENTS

This work was supported by the National Science Foundation, Ceramics Program Grant 1006931. We would like to thank Tina Carvalho (BEMF, UHM) for help with transmission electron microscopy and Ryan Anderson (CalIT2, UCSD) for help with scanning electron microscopy.

REFERENCES

1. Chen, P.Y. and J. McKittrick, *Compressive mechanical properties of demineralized and deproteinized cancellous bone.* Journal of the Mechanical Behavior of Biomedical Materials, **4**(7): p. 961-973. (2011).
2. Novitskaya, E., et al., *Anisotropy in the compressive mechanical properties of bovine cortical bone and the mineral and protein constituents.* Acta Biomaterialia, **7**(8): p. 3170-3177. (2011).
3. Launey, M.E., M.J. Buehler, and R.O. Ritchie, *On the Mechanistic Origins of Toughness in Bone*, in *Annual Review of Materials Research, Vol 40*. 2010, Annual Reviews: Palo Alto. p. 25-53.
4. Bonfield, W., *COMPOSITES FOR BONE-REPLACEMENT.* Journal of Biomedical Engineering, **10**(6): p. 522-526. (1988).
5. Liao, S.S., et al., *Hierarchically biomimetic bone scaffold materials: Nano-HA/collagen/PLA composite.* Journal of Biomedical Materials Research Part B-Applied Biomaterials, **69B**(2): p. 158-165. (2004).
6. Low, K.L., et al., *Calcium phosphate-based composites as injectable bone substitute materials.* Journal of Biomedical Materials Research Part B-Applied Biomaterials, **94B**(1): p. 273-286. (2010).
7. Pielichowska, K. and S. Blazewicz, *Bioactive Polymer/Hydroxyapatite (Nano)composites for Bone Tissue Regeneration*, in *Biopolymers: Lignin, Proteins, Bioactive Nanocomposites*. 2010, Springer-Verlag Berlin: Berlin. p. 97-207.
8. Tenhuisen, K.S., et al., *FORMATION AND PROPERTIES OF A SYNTHETIC BONE COMPOSITE - HYDROXYAPATITE-COLLAGEN.* Journal of Biomedical Materials Research, **29**(7): p. 803-810. (1995).
9. Azevedo, M.C., et al., *Development and properties of polycaprolactone/hydroxyapatite composite biomaterials.* Journal of Materials Science-Materials in Medicine, **14**(2): p. 103-107. (2003).
10. Boeree, N.R., et al., *DEVELOPMENT OF A DEGRADABLE COMPOSITE FOR ORTHOPEDIC USE - MECHANICAL EVALUATION OF AN HYDROXYAPATITE POLYHYDROXYBUTYRATE COMPOSITE-MATERIAL.* Biomaterials, **14**(10): p. 793-796. (1993).
11. Coskun, S., F. Korkusuz, and V. Hasirci, *Hydroxyapatite reinforced poly(3-hydroxybutyrate) and poly(3-hydroxybutyrate-co-3-hydroxyvalerate) based degradable composite bone plate.* Journal of Biomaterials Science-Polymer Edition, **16**(12): p. 1485-1502. (2005).
12. Hao, J.Y., M.L. Yuan, and X.M. Deng, *Biodegradable and biocompatible nanocomposites of poly(epsilon-caprolactone) with hydroxyapatite nanocrystals: Thermal and mechanical properties.* Journal of Applied Polymer Science, **86**(3): p. 676-683. (2002).
13. Hong, Z.K., et al., *Composites of poly(lactide-co-glycolide) and the surface modified carbonated hydroxyapatite nanoparticles.* Journal of Biomedical Materials Research Part A, **81A**(3): p. 515-522. (2007).
14. Misra, S.K., et al., *Polyhydroxyalkanoate (PHA)/inorganic phase composites for tissue engineering applications.* Biomacromolecules, **7**(8): p. 2249-2258. (2006).
15. Neuendorf, R.E., et al., *Adhesion between biodegradable polymers and hydroxyapatite: Relevance to synthetic bone-like materials and tissue engineering scaffolds.* Acta Biomaterialia, **4**(5): p. 1288-1296. (2008).
16. Russias, J., et al., *Fabrication and mechanical properties of PLA/HA composites: A study of in vitro degradation.* Materials Science & Engineering C-Biomimetic and Supramolecular Systems, **26**(8): p. 1289-1295. (2006).
17. Shishatskaya, E.I., I.A. Khlusov, and T.G. Volova, *A hybrid PHB-hydroxyapatite composite for biomedical application: production, in vitro and in vivo investigation.* Journal of Biomaterials Science-Polymer Edition, **17**(5): p. 481-498. (2006).
18. Mygind, T., et al., *Mesenchymal stem cell ingrowth and differentiation on coralline hydroxyapatite scaffolds.* Biomaterials, **28**(6): p. 1036-1047. (2007).
19. Azami, M., F. Moztarzadeh, and M. Tahriri, *Preparation, characterization and mechanical properties of controlled porous gelatin/hydroxyapatite nanocomposite through layer solvent casting combined with freeze-drying and lamination techniques.* Journal of Porous Materials, **17**(3): p. 313-320. (2010).
20. Deville, S., E. Saiz, and A.P. Tomsia, *Freeze casting of hydroxyapatite scaffolds for bone tissue engineering.* Biomaterials, **27**(32): p. 5480-5489. (2006).
21. Fu, Q., et al., *Freeze-cast hydroxyapatite scaffolds for bone tissue engineering applications.* Biomedical Materials, **3**(2): p. 7. (2008).

22. Ramay, H.R. and M.Q. Zhang, *Preparation of porous hydroxyapatite scaffolds by combination of the gel-casting and polymer sponge methods.* Biomaterials, **24**(19): p. 3293-3302. (2003).
23. Swain, S.K., S. Bhattacharyya, and D. Sarkar, *Preparation of porous scaffold from hydroxyapatite powders.* Materials Science & Engineering C-Materials for Biological Applications, **31**(6): p. 1240-1244. (2011).
24. Yang, T.Y., et al., *Hydroxyapatite scaffolds processed using a TBA-based freeze-gel casting/polymer sponge technique.* Journal of Materials Science-Materials in Medicine, **21**(5): p. 1495-1502. (2010).
25. Martinez-Vazquez, F.J., et al., *Improving the compressive strength of bioceramic robocast scaffolds by polymer infiltration.* Acta Biomaterialia, **6**(11): p. 4361-4368. (2010).
26. Miao, X., et al., *Preparation and characterization of interpenetrating phased TCP/HA/PLGA composites.* Materials Letters, **59**(29-30): p. 4000-4005. (2005).
27. Peroglio, M., et al., *Mechanical properties and cytocompatibility of poly(epsilon-caprolactone)-infiltrated biphasic calcium phosphate scaffolds with bimodal pore distribution.* Acta Biomaterialia, **6**(11): p. 4369-4379. (2010).
28. Sharifi, S., et al., *Hydroxyapatite scaffolds infiltrated with thermally crosslinked polycaprolactone fumarate and polycaprolactone itaconate.* Journal of Biomedical Materials Research Part A, **98A**(2): p. 257-267. (2011).
29. Launey, M.E., et al., *Designing highly toughened hybrid composites through nature-inspired hierarchical complexity.* Acta Materialia, **57**(10): p. 2919-2932. (2009).
30. Pezzotti, G., et al., *In situ polymerization into porous ceramics: a novel route to tough biomimetic materials.* Journal of Materials Science-Materials in Medicine, **13**(8): p. 783-787. (2002).
31. Elkasabi, Y., H.Y. Chen, and J. Lahann, *Multipotent polymer coatings based on chemical vapor deposition copolymerization.* Advanced Materials, **18**(12): p. 1521-+. (2006).
32. Chen, Y.G., et al., *Recovery of poly-3-hydroxybutyrate from Alcaligenes eutrophus by surfactant-chelate aqueous system.* Process Biochemistry, **34**(2): p. 153-157. (1999).
33. Hahn, S.K., Y.K. Chang, and S.Y. Lee, *RECOVERY AND CHARACTERIZATION OF POLY(3-HYDROXYBUTYRIC ACID) SYNTHESIZED IN ALCALIGENES-EUTROPHUS AND RECOMBINANT ESCHERICHIA-COLI.* Applied and Environmental Microbiology, **61**(1): p. 34-39. (1995).
34. Jacquel, N., et al., *Isolation and purification of bacterial poly (3-hydroxyalkanoates).* Biochemical Engineering Journal, **39**(1): p. 15-27. (2008).
35. Yu, J., D. Plackett, and L.X.L. Chen, *Kinetics and mechanism of the monomeric products from abiotic hydrolysis of poly[(R)-3-hydroxybutyrate] under acidic and alkaline conditions.* Polymer Degradation and Stability, **89**(2): p. 289-299. (2005).
36. Porter, M. and J. Yu, *Crystallization Kinetics of Poly(3-hydroxybutyrate) Granules in Different Environmental Conditions.* Journal of Biomaterials and Nanobiotechnology, **2**(3): p. 301-310. (2011).
37. Van de Velde, K. and P. Kiekens, *Biopolymers: overview of several properties and consequences on their applications.* Polymer Testing, **21**(4): p. 433-442. (2002).
38. Porter, M. and J. Yu, *Monitoring the in situ crystallization of native biopolyester granules in Ralstonia eutropha via infrared spectroscopy.* Journal of Microbiological Methods, **87**(1): p. 49-55. (2011).
39. Gibson, L.J. and M.F. Ashby, *Cellular Solids: Structure and Properties*. 2 ed., Cambridge: Cambridge University Press (1999).